


# Modulation of the microbiota by oral antibiotics treats immunoglobulin A nephropathy in humanized mice

Jonathan M. Chemouny<sup>1,2,3,4,5</sup>, Patrick J. Gleeson<sup>1,2,3</sup>, Lilia Abbad<sup>1,2,3</sup>, Gabriella Lauriero<sup>1,2,3,6</sup>, Erwan Boedec<sup>1,2,3</sup>, Karine Le Roux<sup>5</sup>, Céline Monot<sup>5</sup>, Maxime Bredel<sup>5</sup>, Julie Bex-Coudrat<sup>1,2,3</sup>, Aurélie Sannier<sup>3,7</sup>, Eric Daugas<sup>1,2,3,4</sup>, Francois Vrtovsnik<sup>1,2,3,4</sup>, Loreto Gesualdo<sup>6</sup>, Marion Leclerc<sup>5</sup>, Laureline Berthelot<sup>1,2,3</sup>, Sanae Ben Mkaddem<sup>1,2,3</sup>, Patricia Lepage<sup>5</sup> and Renato C. Monteiro <sup>1,2,3,4,8</sup>

<sup>1</sup>INSERM 1149, Center for Research on Inflammation (CRI), Paris, France, <sup>2</sup>CNRS ERL8252, Paris, France, <sup>3</sup>Inflamex Laboratory of Excellence, School of Medicine, Paris Diderot University, Sorbonne Paris Cité, Paris, France, <sup>4</sup>Nephrology Department, Bichat-Claude Bernard Hospital, AP-HP, DHU Fire, Paris, France, <sup>5</sup>Institut Micalis, INRA, AgroParisTech, University Paris-Saclay, Jouy-en-Josas, France, <sup>6</sup>Department of Emergency and Organ Transplantation, Division of Nephrology, Dialysis, and Transplantation, University of Bari, Bari, Italy, <sup>7</sup>Pathology Department, Bichat-Claude Bernard Hospital, AP-HP, DHU Fire, Paris, France and <sup>8</sup>Hemato-Immunology Department, UF Immunity Dysfunctions, Bichat-Claude Bernard Hospital, AP-HP, DHU Fire, Paris, France

Correspondence and offprint requests to: Renato C. Monteiro; E-mail: renato.monteiro@inserm.fr

## ABSTRACT

**Background.** Immunoglobulin A nephropathy (IgAN) is the most common primary glomerulonephritis worldwide. IgA is mainly produced by the gut-associated lymphoid tissue (GALT). Both experimental and clinical data suggest a role of the gut microbiota in this disease. We aimed to determine if an intervention targeting the gut microbiota could impact the development of disease in a humanized mouse model of IgAN, the  $\alpha 1^{\text{KI}}$ -CD89<sup>Tg</sup> mice.

**Methods.** Four- and 12-week old mice were divided into two groups to receive either antibiotics or vehicle control. Faecal bacterial load and proteinuria were quantified both at the beginning and at the end of the experiment, when blood, kidneys and intestinal tissue were collected. Serum mouse immunoglobulin G (mIgG) and human immunoglobulin A1 (hIgA1)-containing complexes were quantified. Renal and intestinal tissue were analysed by optical microscopy after haematoxylin and eosin colouration and immunohistochemistry with anti-hIgA and anti-mouse CD11b antibodies.

**Results.** Antibiotic treatment efficiently depleted the faecal microbiota, impaired GALT architecture and impacted mouse IgA production. However, while hIgA1 and mIgG serum levels were unchanged, the antibiotic treatment markedly prevented hIgA1 mesangial deposition, glomerular inflammation and the development of proteinuria. This was associated with a significant decrease in circulating hIgA1–mIgG complexes. Notably, final faecal bacterial load strongly correlated with critical clinical and pathophysiological features of IgAN such as proteinuria and hIgA1–mIgG

complexes. In addition, treatment with broad-spectrum antibiotics reverted established disease.

**Conclusions.** These data support an essential role of the gut microbiota in the generation of mucosa-derived nephrotoxic IgA1 and in IgAN development, opening new avenues for therapeutic approaches in this disease.

**Keywords:** antibiotics, GALT, gut microbiome, IgA, IgA nephropathy

## INTRODUCTION

Immunoglobulin A nephropathy (IgAN) is the most common primary glomerulonephritis worldwide [1]. Most patients diagnosed with this condition are in their third or fourth decade of life [2]. It is estimated that at least 10% of patients with IgAN will require renal replacement therapy within 10 years of diagnosis [3]. IgAN pathophysiology mainly involves abnormally glycosylated IgA1 (galactose-deficient IgA1, Gd-IgA1) [4], which then becomes a target of anti-Tn antigen IgG [5]. IgA1 complexes bind to an IgA Fc receptor (CD89) expressed by monocytes and neutrophils, inducing shedding of this receptor (sCD89) and its integration into the complexes that are elevated in serum of patients with IgAN [6]. Increased serum IgA1–IgG complexes and decreased serum IgA–sCD89 complexes have been shown to be associated with disease progression or recurrence after transplantation [7–9]. IgA1 complexes deposit in the mesangium, where they activate mesangial cells through IgA receptors. Three mesangial IgA receptors have so far been

described: the transferrin receptor, integrin alpha1/beta1 and alpha2/beta1, and 1, 4-galactosyltransferase 1 [10–12]. Among them, the mesangial transferrin receptor (CD71) is strongly upregulated in IgA nephropathy [13], being associated with transglutaminase 2 (TG2) [14]. IgA1 complexes induce CD71 activation leading to kinase phosphorylation and cytokine secretion [15], which may serve as potential factors for other lesions through cross-talk with podocytes [15, 16] and tubular cells [17]. However, the origin of Gd-IgA1 and its mechanisms of production are still incompletely understood, leaving a lack of specific therapeutic targets for IgAN.

In humans, IgA is mainly produced by the mucosa-associated lymphoid tissue (MALT) from where it is secreted into the lumen and participates in the barrier function of the mucosa. Gut-associated lymphoid tissue (GALT) is the most extensive MALT, and therefore the primary source of both subclasses of IgA. A relationship between the digestive tract and IgAN is strongly suggested by its association with inflammatory bowel diseases (which share common genetic risk loci with IgAN) [18] and coeliac disease [19]. The latter shares common pathophysiological mechanisms with IgAN notably by overexpressing CD71 at the apical side of enterocytes associated with TG2 [20, 21]. On the other hand, depletion of gluten in the diet prevents IgAN development in mice humanized for IgA1 and CD89 [22]. This link between the intestine and IgAN has recently been consolidated by three different studies: (i) a genome-wide association study has associated IgAN with polymorphisms of genes involved in gut mucosal immunity [23], (ii) faecal microbiota dysbiosis has been reported in IgAN [24] and (iii) treatment with corticosteroids targeting the gut mucosa protects renal function in patients with IgAN [25].

It is known that not just the intestinal immune system, but also systemic immunity, is largely influenced by antigenic stimulation from the commensal microflora and, more specifically, the intestinal microbiota [26]. Mice overexpressing the B-cell activation factor of the tumour necrosis factor family (BAFF) exhibit an elevation in serum IgA in association with a renal disease that has features similar to IgAN [27]. Under germ-free conditions, these transgenic mice have decreased serum IgA as well as an abolition of glomerular IgA deposits. Similarly, glomerular human IgA1 (hIgA1) deposits are reduced under germ-free conditions, along with a significant reduction in serum IgA1, in mice expressing the human  $\alpha 1$  heavy chain instead of the murine  $\mu$  chain [28]. In both of these models, mice were deprived of stimulation by commensal flora from birth, which prevents normal maturation of the immune system [29].

In the present study, we examined whether microbiota modulation would modify spontaneous IgAN development in a recently described animal model of IgAN induced by transgenic expression of hIgA1 and its specific receptor, human CD89 ( $\alpha 1^{KI}$ -CD89<sup>Tg</sup> mice) [14]. Microbiota modulation was performed by oral antibiotic administration in mice with a developed immune system (4 weeks old) and compared with vehicle control (VC). The results indicate a crucial role of the microbiota and mucosa-derived IgA in the development of IgA nephropathy in this murine model.

## MATERIALS AND METHODS

### *In vivo* experiments

Mice were raised and maintained in a specific pathogen-free mouse facility at the Centre for Research on Inflammation, Paris, France. All experiments were performed in accordance with National Ethics Guidelines and with approval of the Local Ethics Committee (Comité d'Éthique Expérimentation Animale Bichat-Debré). For preventive treatment, mice remained with their mother for suckling until 4 weeks old. Then, littermates were randomly assigned to receive 40  $\mu$ L/g body weight of either a broad-spectrum antibiotic mix [metronidazole (5 mg/mL), neomycin (5 mg/mL), vancomycin (2.5 mg/mL) and amoxicillin (5 mg/mL)] or VC ( $\text{Na}_2\text{HPO}_4 \cdot 12\text{H}_2\text{O}$  1.5 g/L and NaCl 7.4 g/L), twice a week for 8 weeks by oral gavage. For treatment of established disease, 12-week-old male mice were given either broad-spectrum antibiotics (vancomycin 0.5 g/L, metronidazole 1g/L, amoxicillin 1g/L and neomycin 1g/L with 5% sucrose) or VC ( $\text{Na}_2\text{HPO}_4 \cdot 12\text{H}_2\text{O}$  300 mg/L; NaCl 1.48 g/L, 5% sucrose, pH adjusted to 6.5 with citric acid) in their drinking water for 6 weeks. Urine and faeces were collected before starting, and at the end of the treatment protocol. Blood was collected by cardiac puncture and mice were sacrificed by cervical dislocation. Kidneys and small intestine containing Peyer's patches (PP) were collected. Organs were conserved in either OCT (CML, Nemours, France) or formalin 10% (Sigma-Aldrich, Saint-Quentin Fallavier, France).

To test the effect of broad-spectrum antibiotics on adaptive immunity, 4-week-old  $\alpha 1^{KI}$ -CD89<sup>Tg</sup> mice were given broad-spectrum antibiotics or VC in their drinking water for 5 weeks and were then immunized with 0.5 mg of rabbit IgG in 500  $\mu$ L of Complete Freund's Adjuvant (Sigma F5881) or phosphate-buffered saline alone. Antibiotics or VC were continued for a further 10 days before serum was collected from the retro-orbital sinus.

### Faecal bacterial load quantification and composition assessment

Mouse stool samples were collected in a sterile tube, aliquoted (150 mg), and DNA was extracted using both mechanical and chemical lysis as described [30]. DNA was extracted according to International Human Microbiome Standards SOP07 ([http://www.microbiome-standards.org/fileadmin/SOPs/IHMS\\_SOP\\_07\\_V2.pdf](http://www.microbiome-standards.org/fileadmin/SOPs/IHMS_SOP_07_V2.pdf)). Quantitative PCR targeting the Bacteria domain (Eubacteria Eub338 probe) was performed to analyse bacterial loads. The microbiota composition and diversity was determined by MiSeq sequencing (Illumina) of the V3-V4 region of the 16S rRNA genes.

### Histological procedures

Paraffin-embedded, 4  $\mu$ m sections of intestine and kidney were stained with haematoxylin-eosin for morphological analysis. For immunohistochemistry, 4  $\mu$ m sections of cryostat frozen intestine or kidney were fixed in acetone, incubated for 1 h in 5% bovine serum albumin (Euromedex, Souffelweyersheim, France), followed by 1 h 30 min at room temperature with

biotinylated mouse anti-hIgA (Catalogue number 555884) for gut and kidney or anti-mouse CD11b (Catalogue number 553309) for kidney only (both from BD Biosciences, Le Pont de Claix, France). Detection was performed with vectastain elite ABCkit (Vector, Burlingame, CA, USA). Immunofluorescence staining was performed on frozen sections with goat anti-hIgA-FITC (1/100, Southern Biotech). Slides were mounted with Immuno-mount (Thermo Fisher Scientific) and read with an upright microscope, DM2000 (Leica, Wetzlar, Germany) at  $\times 400$  magnification using IM50 software (Leica) or an immunofluorescent microscope (Zeiss LSM 780). Quantification of hIgA1-positive intestinal gut was performed by counting the number of hIgA1-positive cells in the intestinal mucosa for each section at  $\times 400$  magnification and dividing by the total number of individual fields required to cover the entire section. Quantification of glomerular cellularity and CD11b-positive cells was performed by counting the number of nuclei/CD11b-positive cells in 20 randomly chosen glomeruli for each mouse. Glomerular area positive for hIgA1 was reported as the area positive for hIgA1 as a percentage of the total area of the glomerulus as measured using ImageJ as previously described [22], or the fluorescence intensity as measured with Imaris 7.2 software (Bitplane).

### Enzyme-linked immunosorbent assay

Serum levels of hIgA and mIgG were assessed with the corresponding Bethyl quantification (E88-102 and E90-131, respectively) set according to the manufacturer's instructions. Regarding hIgA1 complexes, serum complexes were isolated using polyethylene glycol precipitation. Measurement of hIgA1-mIgG and hIgA1-sCD89 complexes were determined with a sandwich enzyme-linked immunosorbent assay (ELISA) [31]. Anti-hIgA (Bethyl Laboratories, 10  $\mu\text{g}/\text{mL}$ ) or A3 mAb anti-human CD89 (10  $\mu\text{g}/\text{mL}$ ) was used for coating. Precipitated sera (1:5 diluted) were then added and revealed with anti-mIgG (1:5000 dilution) or anti-hIgA (1:2000 dilution) coupled with alkaline phosphatase (Southern Biotech, Birmingham, AL, USA). The optic density (OD) at 405 nm was measured after the addition of alkaline phosphatase substrate (Sigma-Aldrich). The complex levels were expressed as OD.

Generation of mouse anti-rabbit IgG antibodies was measured in serum using a sandwich ELISA method. A plate was coated with rabbit IgG (5 mcg/mL) or goat IgG (isotype control; 5 mcg/mL) in parallel duplicate columns. After incubation with diluted mouse serum, wells were washed, then incubated with anti-mouse IgG-horseradish peroxidase (HRP) (Bethyl) and revealed with TMB substrate. OD values obtained from wells coated with goat IgG were subtracted as background for each mouse.

### Statistical analysis

Statistical analyses were performed using RStudio integrated development environment for R (RStudio, Inc., Boston, MA, USA). Comparisons between numerical variables were performed using Wilcoxon's sum-rank test. Categorical variables were compared using Fisher's exact test. Correlations were analysed with Spearman's test. Effect of treatment on mice weight gain was analysed with a likelihood ratio test. Effect of

treatment on faecal bacterial load reduction and proteinuria was analysed using a mixed-effect model with random-effect attributed to mice and fixed-effect to treatment group and time.

## RESULTS

### Antibiotic treatment depletes gut microbiota without liver and renal toxicity

In order to deplete the microbiota, we subjected 4-week-old  $\alpha 1^{\text{KI}}\text{-CD89}^{\text{Tg}}$  mice to either VC ( $n = 15$ ) or broad-spectrum antibiotics (ATB) ( $n = 16$ ) by oral gavage for 8 weeks (Figure 1A). Five mice died during the experiment (two in the ATB group and three in the VC group,  $P > 0.1$ , data not shown). ATB treatment resulted in an effective depletion ( $P < 0.001$ ) of the mouse gut microbiota as compared with VC (Figure 1B). There was one mouse in the ATB group in which depletion of faecal bacterial load was not achieved, so it was excluded from analyses despite decreased proteinuria at the end of the protocol and a similar microbiota composition to other mice treated with ATB (Supplementary data, Figure S1). Compared with the samples collected at 4 weeks old, before initiation of the protocol, faecal bacterial load was reduced to  $613.0 \pm 236.7$ -fold at the end of the experiment in the ATB group as compared with  $1.5 \pm 1.1$ -fold in the VC group. Antibiotic treatment resulted in significantly less weight gain ( $P < 0.001$ ) with a final weight (mean  $\pm$  SD) of  $23.2 \pm 2.6$  g in the ATB group and  $26.5 \pm 3.5$  g in the VC group (Figure 1C). No evidence of liver or renal toxicity was detected: there were no significant difference between groups in bilirubin, alkaline phosphatase, aspartate aminotransferase (AST) or serum creatinine (Figure 1D–G,  $P > 0.1$ ). Furthermore, serum creatinine levels of these  $\alpha 1^{\text{KI}}\text{-CD89}^{\text{Tg}}$  mice were similar to those of wild type mice of the same age (Supplementary data, Figure S2).

### Microbiota depletion abolishes the IgA nephropathy phenotype

Twelve-week-old  $\alpha 1^{\text{KI}}\text{-CD89}^{\text{Tg}}$  mice spontaneously develop mesangial hIgA1 deposition, along with proteinuria, mimicking IgA nephropathy as described previously [14]. Anti-hIgA immunostaining of mouse kidney revealed that hIgA1 deposition was significantly reduced ( $P = 0.008$ ) in ATB mice compared with VC mice (Figure 2A and C). At twelve-weeks old, mice in the VC group developed proteinuria [initial and final urinary protein-to-creatinine ratio (UPCR)  $0.7 \pm 0.2$  and  $3.7 \pm 0.4$  g/mmol, respectively], in keeping with our previous report of this model [14]. Conversely, antibiotic-treated mice were protected from renal disease (initial and final UPCR  $0.8 \pm 0.2$  and  $0.8 \pm 0.1$  g/mmol). Antibiotics significantly affected the development of proteinuria over time ( $P < 0.001$ , Figure 2B). These results were confirmed in an additional experiment using a different protocol where the mice's drinking water was supplemented with broad-spectrum antibiotics for 12 weeks (Supplementary data, Figure S3). Additionally, antibiotics prevented the development of glomerular inflammation as illustrated by fewer glomeruli with infiltrating CD11b-positive cells ( $P = 0.008$ , Figure 2D and E) despite a similar number of cells in the glomeruli of both groups ( $P = 0.157$ , Figure 2E). It is

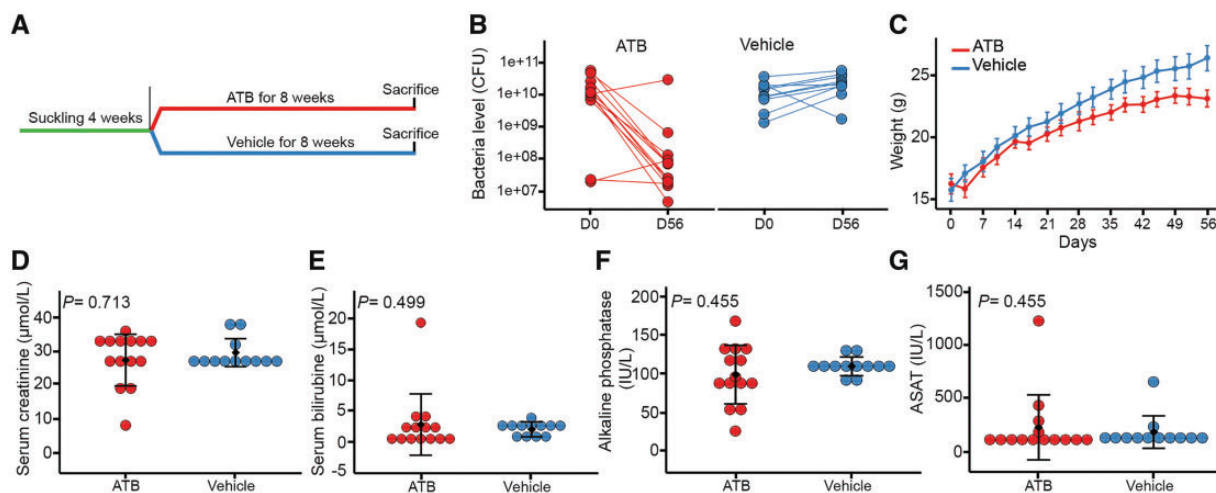


**FIGURE 1:** The attenuated antibiotic protocol efficiently depletes the faecal microbiota without toxicity. (A) Four-week-old mice were given 40  $\mu$ L/g of either an antibiotic mix (metronidazole 5 mg/mL, neomycin 5 mg/mL, vancomycin 2.5 mg/mL and amoxicillin 5 mg/mL) or a vehicle ( $\text{Na}_2\text{HPO}_4 \cdot 12\text{H}_2\text{O}$  1.5 g/L and NaCl 7.4 g/L) by oral gavage twice a week for 8 weeks before sacrifice. (B) Faeces were collected at the beginning and the end of the experiment and the faecal bacterial load was quantified by qPCR targeting the Bacteria domain (Eubacteria Eub338 probe) (bacteria/g faeces). Effect of the treatment on faecal microbiota depletion was analysed with a linear mixed model. (C) Mice were weighed before each gavage twice a week through the experimental protocol. Effect of the treatment on weight gain was done with a likelihood ratio test. (D–G) Serum creatinine ( $\mu\text{mol/L}$ ), serum bilirubin ( $\mu\text{mol/L}$ ), alkaline phosphatase (IU/L) and aspartate aminotransferase (ASAT, IU/L) at the end of the experiment for mice that received antibiotics or vehicle and compared using Wilcoxon's test. CFU, colony-forming units.

noteworthy that antibiotic treatment reduced the formation of hIgA1–mIgG complexes ( $P = 0.002$ , Figure 3A), one of the major hallmarks of the disease, independently of hIgA1 ( $\rho = -0.232$ ,  $P = 0.352$ , Supplementary data, Figure S4A) or mIgG serum levels ( $\rho = 0.007$ ,  $P = 0.980$ , Supplementary data, Figure S4B). Conversely, serum levels of hIgA–sCD89 complexes were similar in the ATB and the VC group ( $P = 0.564$ , Figure 3B).

We next addressed whether long-term broad-spectrum antibiotic treatment could reverse overt IgA nephropathy in our humanized mouse model. Twelve-week-old  $\alpha 1^{\text{KI}}\text{-CD89}^{\text{Tg}}$  mice with established disease were given drinking water supplemented with broad-spectrum antibiotics ( $n = 4$ ) or VC ( $n = 4$ ) for 6 weeks. Although all mice exhibited significant proteinuria at the beginning of the experiment, mice treated with antibiotics displayed a marked reduction of proteinuria as opposed to mice who received VC only (Figure 4A,  $P < 0.001$ ) consistent with a decrease in faecal bacterial load after antibiotic treatment (Figure 4B,  $P = 0.029$ ). Moreover, hIgA1 glomerular deposits and glomerular infiltration with CD11b+ cells were significantly reduced in mice treated with antibiotics as compared with vehicle ( $P = 0.01$  and  $0.03$ , respectively) as illustrated in Figure 4C and D.

### Microbiota depletion alters GALT structure, but not serum hIgA1 production

As germ-free mice display impaired adaptive immune function, including decreased circulating immunoglobulin levels, we evaluated the effect of a microbiota-depleting antibiotic protocol on circulating hIgA1 levels and GALT. For this purpose, we first collected all thickened portions of the small intestine suspected to contain PP. Light microscopy visualization of small intestine revealed the presence of lymphoid structures in eight (67%) VC mice and three (23%) ATB mice ( $P = 0.047$ ,

Figure 5A). In addition, lymphoid structures identified in ATB mice had altered architecture (Figure 5B). Immunostaining of intestinal tissue with anti-hIgA did not reveal any differences in the number of hIgA1+ cells ( $P = 0.784$ , Figure 5C) or in the staining pattern (Figure 5D), suggesting that homing of hIgA1 producing plasma cells into the submucosa was not impaired in our model. Moreover, antibiotic treatment did not alter the adaptive immune response, as demonstrated by an antigen challenge experiment (Supplementary data, Figure S5). In agreement with these results, mice given either ATB or VC displayed similar serum levels of hIgA1 ( $401 \pm 37$  and  $359 \pm 54$  mg/L, respectively,  $P = 0.316$ ). Circulating murine IgG levels were also similar in both groups (ATB:  $130 \pm 17$  and VC:  $122 \pm 14$  mg/L,  $P = 0.979$ ).

### Gut microbiota is associated with clinical and pathophysiological features of IgA nephropathy

To demonstrate a relationship between microbiota depletion and the prevention of IgAN, rather than a direct effect of antibiotics on glomerular injury, we analysed the relationship between faecal bacterial load and serum immunoglobulin levels, circulating IgA-immune complexes and proteinuria. Final faecal bacterial load did not correlate with hIgA1 ( $\rho = -0.123$ ,  $P = 0.556$ , Supplementary data, Figure S6A) or mIgG serum levels ( $\rho = -0.054$ ,  $P = 0.798$ , Supplementary data, Figure S6B). In contrast, final faecal bacterial load did correlate with UPCR ( $\rho = 0.644$ ,  $P = 0.001$ , Figure 6A) and hIgA1–mIgG complexes ( $\rho = 0.581$ ,  $P = 0.016$ , Figure 6B), but not with hIgA1–sCD89 complexes ( $\rho = 0.262$ ,  $P = 0.308$ , Figure 6C). hIgA1–mIgG complexes also correlated significantly with UPCR ( $\rho = 0.571$ ,  $P = 0.023$ , Figure 6D).

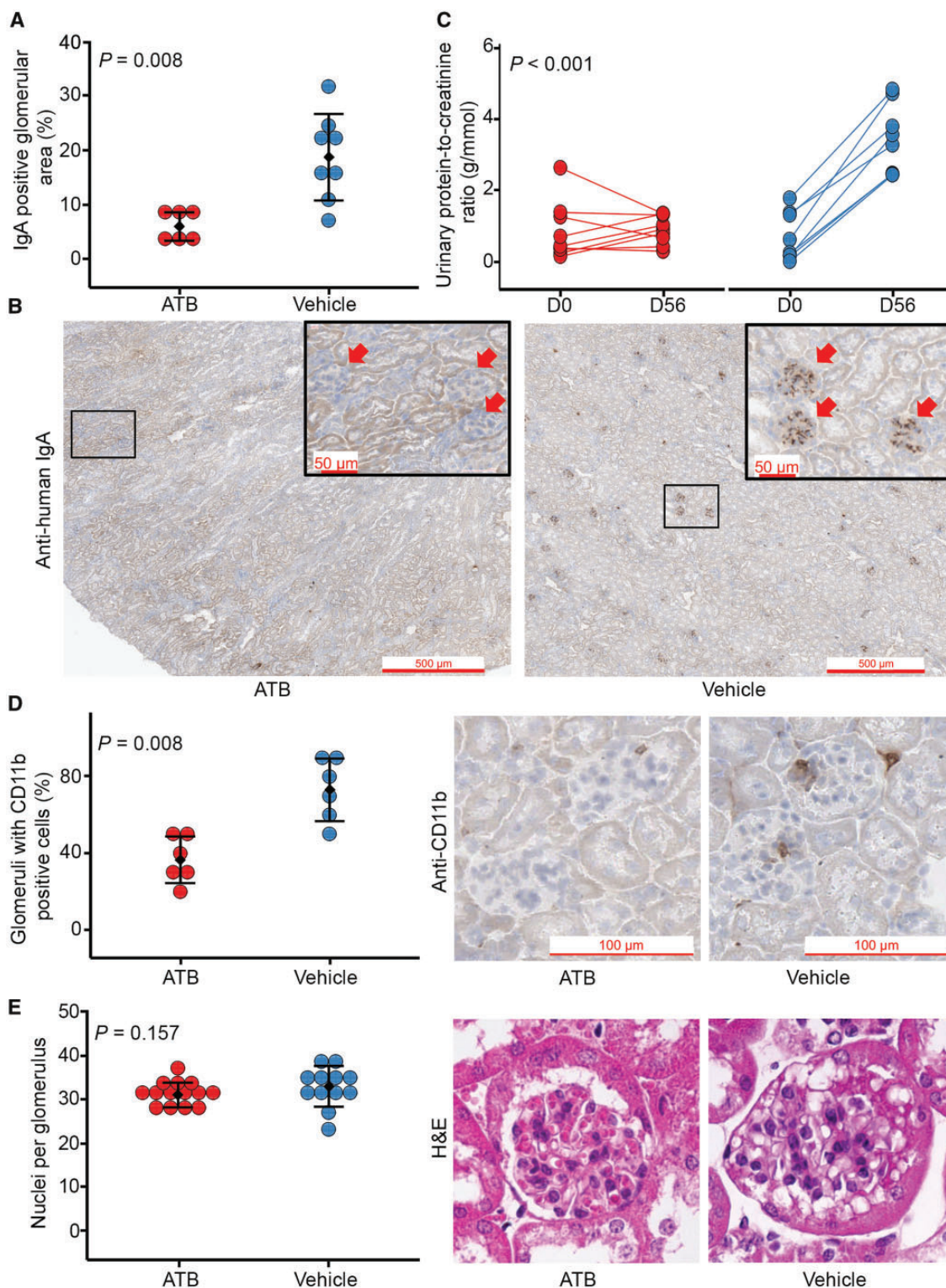


**FIGURE 2:** Antibiotic treatment prevents IgAN in  $\alpha 1^{KI}$ -CD89<sup>Tg</sup> mice. (A) Quantification of immunostaining for hIgA1 in frozen kidney sections of mice that received antibiotics or vehicle (percentage of positive glomerular area) as measured by ImageJ. (B) Representative sections of kidney sections after immunostaining for hIgA1 in mice receiving antibiotics or vehicle (original magnification  $\times 50$ , insert  $\times 200$ ). (C) UPCR at the beginning and the end of the experiment (g/mmol) in mice that received antibiotics or vehicle. Effect of the treatment on the development of proteinuria was analysed with a linear mixed model. (D) Quantification of immunostaining for murine CD11b in frozen kidney sections from mice that received antibiotic mix or vehicle (percentage of glomeruli with CD11b positive cells) as measured by ImageJ (left panel). Representative sections of kidney sections after immunostaining for murine CD11b from mice that received antibiotics or vehicle are shown (right panels, original magnification  $\times 400$ ). (E) Nuclei were counted in 20 randomly chosen glomeruli for each mouse that received either antibiotics or vehicle (nuclei/glomerulus) and compared using Wilcoxon's test (left panels). Representative glomeruli of mice that received antibiotics or vehicle are shown (right panels, original magnification  $\times 400$ ).

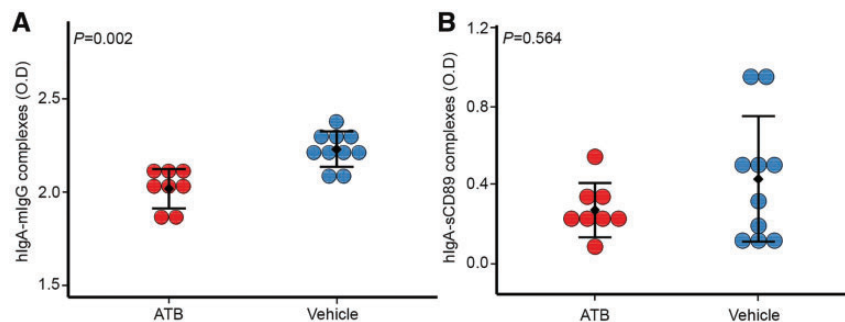


**FIGURE 3:** Antibiotic treatment decreases the formation of hIgA–mIgG but not hIgA–sCD89 complexes. (A) Levels of hIgA–mIgG complexes in mice that received antibiotics or vehicle. (B) IgA1–sCD89 complexes measured by ELISA in mice that received antibiotics or vehicle and compared with Wilcoxon’s test. Anti-hIgA or A3 monoclonal-antibody anti-human CD89 was used for coating. Polyethylene glycol precipitated sera were then added; detection with anti-hIgG or anti-hIgA-HRP. Serum hIgA1 and mIgG levels were measured by ELISA. Statistical analyses performed using Wilcoxon’s test.

## DISCUSSION

Here, we present data that demonstrate an important role of the gut microbiota in disease development in the  $\alpha 1^{KI}$ -CD89<sup>Tg</sup> mouse model of IgAN, which is consistent with the findings of recent clinical studies. The advantage of our model over previously described axenic models is that we were able to study the effect of microbiota modulation in mice with a mature immune system. Our results implicate the intestinal microbiota in the formation of IgA1–IgG immune complexes, a crucial determinant of IgAN pathogenesis. Given the current lack of specific therapies for IgAN, these results open up promising new avenues of investigation for treatments that target the microbiota and provide a new, easily workable, model that can be used to experiment further with the role of the microbiota in IgAN.

IgAN pathogenesis, as the name implies, is dependent on the formation of aberrant IgA1 and IgA1 immune complexes [32]. Our data suggest that these pathogenic forms of IgA are being generated at the mucosa where MALT, the principal producer of IgA, is found, and where IgA plays its principal immunological role. Early development of the immune system, and more particularly of MALT, is largely dependent on antigenic stimulation by antigens from commensal bacteria and reciprocally, the composition of the commensal microbiota depends on MALT function [26, 29]. This results in dynamic cross-talk and equilibrium is achieved when there is a healthy symbiosis between microbiota and host. However, a problem with either the immune or the microbiological component of this system may occur, leading to a disease-associated dysbiosis [33], as has been reported in IgAN [24]. However, the ‘chicken or egg’ question remains, as to whether the altered microbiota is a cause or effect of the disease. Our results, showing prevention of IgAN by depletion of the microbiota from 4 weeks to 12 weeks old, and reversal of established disease by depletion of the microbiota from 12 weeks to 18 weeks, supports a causal role of an intestinal microbial dysbiosis in IgAN. Indeed, microbiota depletion in these mice completely abrogated hIgA1 deposition and prevented the development of proteinuria, as compared with mice that were given VC. If alterations in the microbiota, as reported from clinical studies, were an effect of the disease rather than a cause of the disease, we would not anticipate these dramatic

effects on glomerular IgA1 deposition when the microbiota is depleted by antibiotic therapy.

Two previous studies have analysed the relationship between bacterial environment and disease development in IgAN mouse models. In both instances, breeding the mice under germ-free conditions prevented the disease. However, this axenic approach was also associated with an impairment of immune system maturation and, notably, an important decrease in circulating levels of immunoglobulins that are found deposited in the glomeruli of the respective models (mIgA in the BAFF model [27] and hIgA1 the  $\alpha 1KI$  model [28]). By contrast, here, mice given antibiotics after weaning displayed hIgA1 serum levels similar to their vehicle-treated littermates, and there was no difference between groups in circulating IgG levels, suggesting that systemic immune system maturation was not impaired by microbiota depletion. Moreover, although microbiota depletion altered GALT architecture, it did not affect hIgA1–producing cells or response to systemic immunisation.

Our treatment protocols involved antibiotic administration either twice per-week by gavage or continuously in drinking water, with high doses of broad-spectrum antibiotics. The antibiotic mix contained compounds that are absorbed (amoxicillin and metronidazole) and not absorbed (vancomycin and neomycin) from the gut. The systemically absorbed antibiotics would have also affected the extra-digestive commensal microbiota (e.g. lung). The composition of salivary microbiota from European patients with IgAN was shown to differ from that of healthy controls [34], although no significant difference was found between the tonsillar microbiota of Asian adult patients with IgAN and those with recurrent tonsillitis [35]. Due to the invasive nature of sample collection for the Asian tonsillar study, a healthy adult control group was not possible, making the results ambiguous, as the possibility of a tonsillar dysbiosis common to patients with IgAN and recurrent tonsillitis is not excluded. Interestingly, in our study, faecal bacterial load correlated with proteinuria, supporting the role of bacterial stimulation of mucosal immunity in IgAN pathogenesis, and consistent with the clinical observation of IgAN exacerbated by ear and throat infections. Moreover, final faecal bacterial load correlated with hIgA1–mIgG complex serum levels, but not with hIgA1 or mIgG levels. This demonstrates that: (i) the

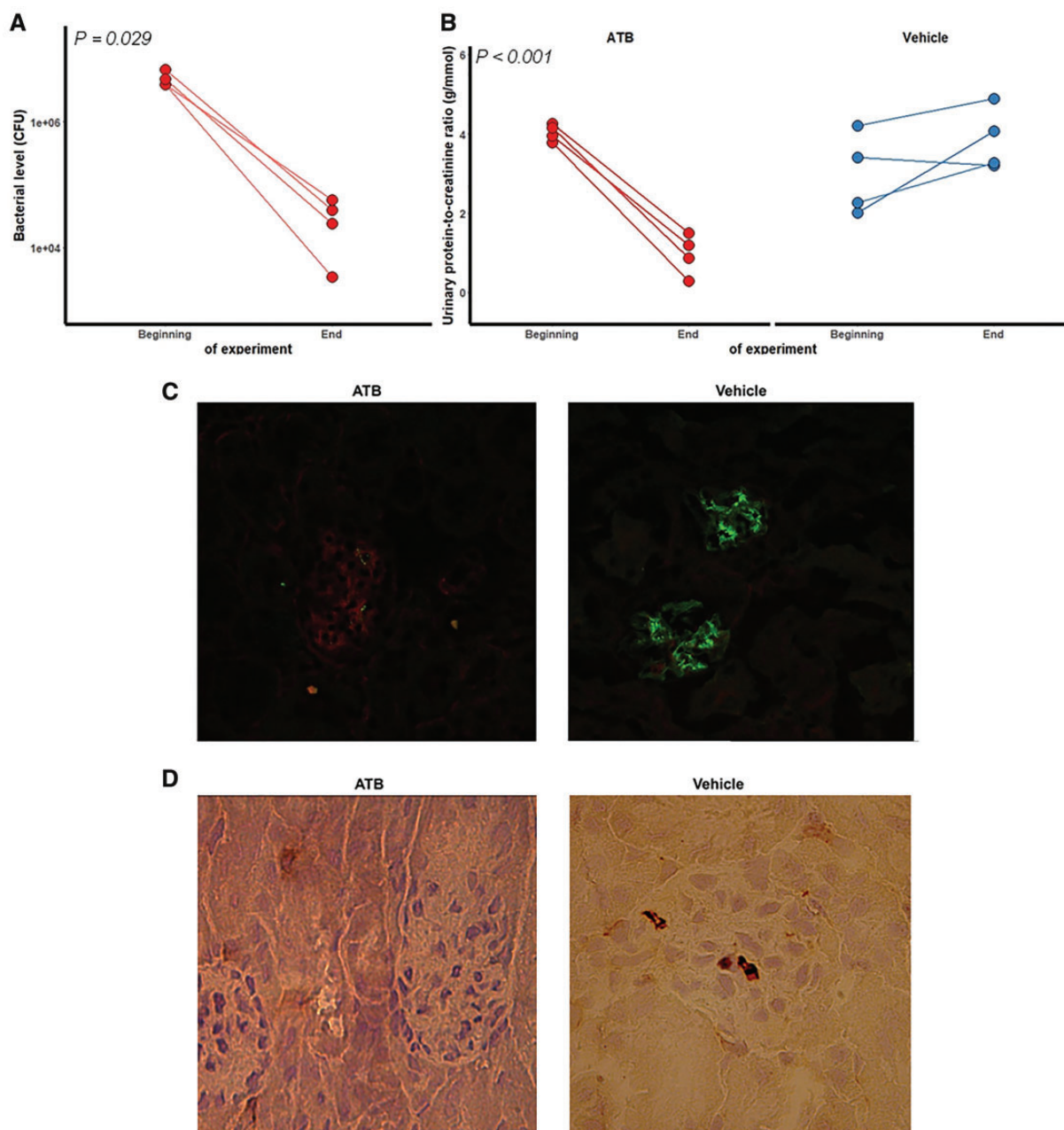


**FIGURE 4:** Broad-spectrum antibiotic treatment reverses overt IgA nephropathy in  $\alpha 1^{KI}$ -CD89<sup>Tg</sup> model. Twelve-week-old mice had their drinking water supplemented with either VC or an antibiotic (ATB) mix (Vancomycin 0.5 g/L, Neomycin 1 g/L, Amoxicillin 1 g/L, Metronidazole 1 g/L with 50 g of sucrose per litre (5%)) for 6 weeks before sacrifice. (A) Faeces were collected at the beginning and the end of the experiment and the faecal bacterial load was quantified by qPCR targeting the Bacteria domain (Eubacteria Eub338 probe) (bacteria/g faeces). Effect of the treatment on faecal microbiota depletion was analysed with a paired Wilcoxon's test. (B) UPCR at the beginning and the end of the experiment (g/mmol) in mice that received antibiotics or vehicle alone. Effect of the treatment on the development of proteinuria was analysed with a linear mixed model. (C and D) Representative sections of kidneys after immunostaining with (C) anti-hIgA-FITC antibody and phalloidin-Alexaflour 568 to delineate glomerular structures (green anti-hIgA1, red phalloidin) and (D) anti-murine CD11b in mice that received antibiotics or vehicle (original magnification  $\times 630$ ). CFU, colony-forming units.

disease phenotype of  $\alpha 1^{KI}$ -CD89<sup>Tg</sup> mice depends on the formation of IgA1-IgG complexes, a key pathophysiological feature of human IgAN and (ii) the formation of these complexes is promoted by the presence of intestinal bacteria, independently of the circulating levels of either of their components.

Given that circulating levels of hIgA1 and the number of hIgA1-positive B cells in the lamina propria did not differ between groups, the protective effect of microbiota depletion

may be mediated through a reduction in the production of anti-Tn antigen-specific IgG, an effect on IgA glycosylation or by reducing an effect of bacterial antigens on immune complex formation. Deposition of streptococcal M protein in the glomeruli of patients with IgAN has been described [36]; together with our results, this suggests that bacterial antigens might promote the formation of these nephrotoxic immune complexes.

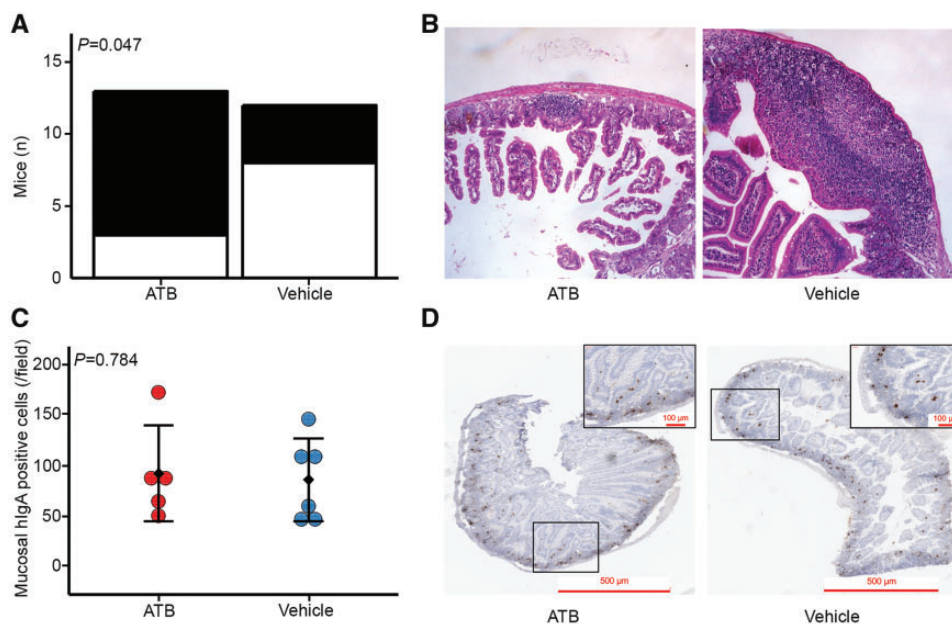


**FIGURE 5:** Antibiotic treatment induces GALT alterations but does not modify the number of IgA-producing cells. Thicker portions of the intestine were collected as potentially harbouring PP, fixed in formalin 4% and included in paraffin. Sections were cut until a lymphoid follicle was identified or the paraffin-embedded sample was exhausted. (A) Number of mice in each group in which lymphoid follicles were identified (black columns indicate no identified lymphoid follicle and white columns presence of identified lymphoid follicle). (B) Representative photomicrography of lymphoid follicles identified in mice given antibiotics (left panel) or vehicle (right panel) (Original magnification  $\times 200$ ). (C) Quantification of immunostaining for hIgA1 in frozen small bowel sections of mice given antibiotics or vehicle (number of positive cells per field). (D) Representative sections of small bowel sections after immunostaining for hIgA1 of mice given antibiotics or vehicle (original magnification  $\times 100$ , inset  $\times 200$ ).

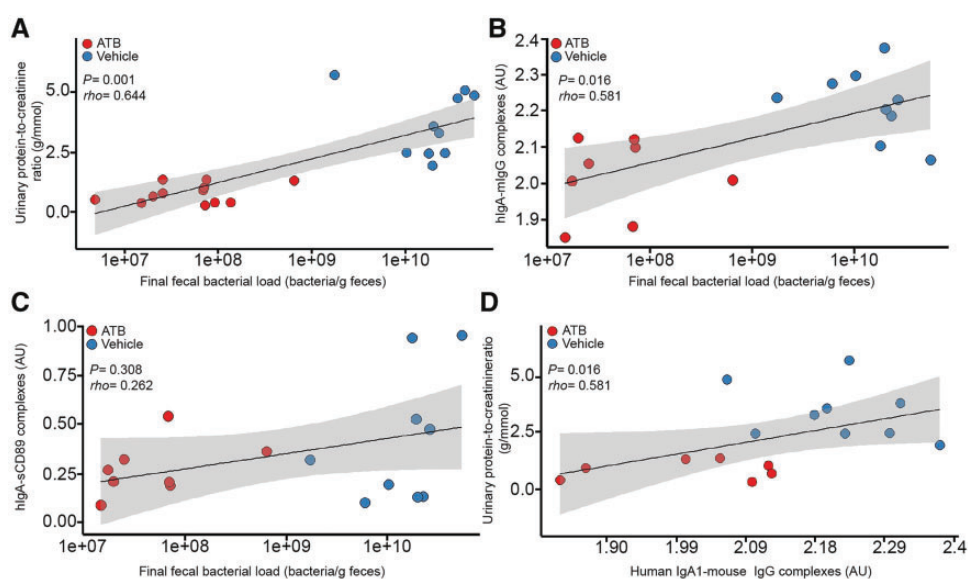


**FIGURE 6:** Final faecal bacterial load correlates with clinical and pathophysiological features of IgAN. Correlation of faecal bacterial load as determined by qPCR targeting the Bacteria domain (Eubacteria Eub338 probe) (bacteria-colony-forming units/g faeces) and (A) UPCR (g/mmol), (B) hIgA1-mIgG complexes (AU), (C) hIgA1-sCD89 complexes (AU) and (D) correlation of hIgA1-mIgG complexes (AU) with UPCR (g/mmol) analysed with Spearman's rank correlation test.

The total faecal bacterial load did not decrease in one of the mice treated with antibiotics; however, this mouse benefited from a reduction in proteinuria nevertheless and was found to have a microbiota composition similar to other antibiotic treated mice. This suggests that changes in microbiota composition are more important than absolute bacterial load in the

prevention of IgAN in our model. One may hypothesize that binding of bacterial antigens by polymeric IgA in the gut lumen and subsequent retrotranscytosis of these immune complexes, as described for coeliac disease [20, 21], could play a role in disease pathogenesis. These complexes, after passing to the basolateral side of the mucosal epithelium, could be recognized and



bound by IgG. A decreased alpha-diversity induced by antibiotics would limit the amount of antigens available to be recognized by IgG and reduce the formation of IgA–IgG complexes.

In conclusion, the data presented here strongly support a causative role of commensal bacteria in the pathophysiology of IgAN and suggest that the microbiota is a candidate therapeutic target. It would not be feasible to give the broad-spectrum antibiotic mix employed in this experiment to patients in the long-term; however, other interventions targeting the microbiota, and more specifically the gut commensal flora, are available. It is possible to modulate the microbiota through dietary interventions, such as: a gluten-free diet [37], which we have shown to prevent IgAN in  $\alpha 1^{KI}$ -CD89<sup>Tg</sup> mice [22]; through administration of probiotics or prebiotics; or, more comprehensively, by faecal transplantation, which has been shown to be efficient in treating *Clostridium difficile*-associated disease [38]. The approach described here, using mice with a mature immune system, should facilitate further proof-of-concept studies into the effects of microbiota modulation on IgAN phenotype, and ultimately give insight into ways to restore symbiosis in dysbiotic patients with IgAN.

## SUPPLEMENTARY DATA

Supplementary data are available at [ndt](http://ndt.oxfordjournals.org/) online.

## ACKNOWLEDGEMENTS

We thank Melissa Pierre and Dr Agnès Jamin for their technical assistance, Nathalie Ialy-Radio for animal breeding, Olivier Thibaudeau and Sofiane Ameur at the Bichat histology platform and Nicolas Sorhaindo at the CRI Biochemistry platform. We acknowledge the INRA @bridge platform for sequencing and we are grateful to the INRA MIGALE bioinformatics platform (<http://migale.jouy.inra.fr>) for providing computational resources.

## FUNDING

This work was funded by Equipe Fondation pour la Recherche Médicale, LABEX Inflammex (ANR-11-IDEX-0005-02), Agence Nationale pour la Recherche Jeune Chercheur TRAIN, Département hospitalo-universitaire FIRE projet Emergence et Association pour l'Information et la Recherche sur les maladies Rénales Génétiques–France. The authors thank the HUPNVS of Assistance Publique - Hôpitaux de Paris for funding publications fees.

## CONFLICT OF INTEREST STATEMENT

None declared.

## REFERENCES

- Wyatt RJ, Julian BA. IgA nephropathy. *N Engl J Med* 2013; 368: 2402–2414
- Nair R, Walker PD. Is IgA nephropathy the commonest primary glomerulopathy among young adults in the USA? *Kidney Int* 2006; 69: 1455–1458

- Coppo R, Troyanov S, Bellur S *et al.* Validation of the Oxford classification of IgA nephropathy in cohorts with different presentations and treatments. *Kidney Int* 2014; 86: 828–836
- Tomana M, Novak J, Julian BA *et al.* Circulating immune complexes in IgA nephropathy consist of IgA1 with galactose-deficient hinge region and anti-glycan antibodies. *J Clin Invest* 1999; 104: 73–81
- Suzuki H, Fan R, Zhang Z *et al.* Aberrantly glycosylated IgA1 in IgA nephropathy patients is recognized by IgG antibodies with restricted heterogeneity. *J Clin Invest* 2009; 119: 1668–1677
- Launay P, Grossetete B, Arcos-Fajardo M *et al.* Fc $\alpha$  receptor (CD89) mediates the development of immunoglobulin A (IgA) nephropathy (Berger's disease). Evidence for pathogenic soluble receptor-IgA complexes in patients and CD89 transgenic mice. *J Exp Med* 2000; 191: 1999–2009
- Vuong MT, Hahn-Zoric M, Lundberg S *et al.* Association of soluble CD89 levels with disease progression but not susceptibility in IgA nephropathy. *Kidney Int* 2010; 78: 1281–1287
- Berthoux F, Suzuki H, Thibaudin L *et al.* Autoantibodies targeting galactose-deficient IgA1 associate with progression of IgA nephropathy. *J Am Soc Nephrol* 2012; 23: 1579–1587
- Berthelot L, Robert T, Vuiblet V *et al.* Recurrent IgA nephropathy is predicted by altered glycosylated IgA, autoantibodies and soluble CD89 complexes. *Kidney Int* 2015; 88: 815–822
- Moura IC, Centelles MN, Arcos-Fajardo M *et al.* Identification of the transferrin receptor as a novel immunoglobulin (Ig)A1 receptor and its enhanced expression on mesangial cells in IgA nephropathy. *J Exp Med* 2001; 194: 417–425
- Kaneko Y, Otsuka T, Tsuchida Y *et al.* Integrin  $\alpha 1/\beta 1$  and  $\alpha 2/\beta 1$  as a receptor for IgA1 in human glomerular mesangial cells in IgA nephropathy. *Int Immunol* 2012; 24: 219–232
- Molyneux K, Wimbury D, Pawluczyk I *et al.*  $\beta 1$ , 4-galactosyltransferase 1 is a novel receptor for IgA in human mesangial cells. *Kidney Int* 2017; 92: 1458–1468
- Haddad E, Moura IC, Arcos FM *et al.* Enhanced expression of the CD71 mesangial IgA1 receptor in Berger disease and Henoch-Schonlein nephritis: association between CD71 expression and IgA deposits. *J Am Soc Nephrol* 2003; 14: 327–337
- Berthelot L, Papista C, Maciel TT *et al.* Transglutaminase is essential for IgA nephropathy development acting through IgA receptors. *J Exp Med* 2012; 209: 793–806
- Tamouza H, Chemouny JM, Raskova Kafkova L *et al.* The IgA1 immune complex-mediated activation of the MAPK/ERK kinase pathway in mesangial cells is associated with glomerular damage in IgA nephropathy. *Kidney Int* 2012; 82: 1284–1296
- Coppo R, Fonsato V, Balegno S *et al.* Aberrantly glycosylated IgA1 induces mesangial cells to produce platelet-activating factor that mediates nephron loss in cultured podocytes. *Kidney Int* 2010; 77: 417–427
- Chan LY, Leung JC, Tsang AW *et al.* Activation of tubular epithelial cells by mesangial-derived TNF- $\alpha$ : glomerulotubular communication in IgA nephropathy. *Kidney Int* 2005; 67: 602–612
- Ambruzs JM, Walker PD, Larsen CP. The histopathologic spectrum of kidney biopsies in patients with inflammatory bowel disease. *Clin J Am Soc Nephrol* 2014; 9: 265–270
- Welander A, Sundelin B, Fored M *et al.* Increased risk of IgA nephropathy among individuals with celiac disease. *J Clin Gastroenterol* 2013; 47: 678–683
- Matysiak-Budnik T, Moura IC, Arcos-Fajardo M *et al.* Secretory IgA mediates retrotranscytosis of intact gliadin peptides via the transferrin receptor in celiac disease. *J Exp Med* 2008; 205: 143–154
- Lebreton C, Menard S, Abed J *et al.* Interactions among secretory immunoglobulin A, CD71, and transglutaminase-2 affect permeability of intestinal epithelial cells to gliadin peptides. *Gastroenterology* 2012; 143: 698–707 e4
- Papista C, Lechner S, Ben Mkaddem S *et al.* Gluten exacerbates IgA nephropathy in humanized mice through gliadin-CD89 interaction. *Kidney Int* 2015; 88: 276–285
- Kiryuluk K, Li Y, Scolari F *et al.* Discovery of new risk loci for IgA nephropathy implicates genes involved in immunity against intestinal pathogens. *Nat Genet* 2014; 46: 1187–1196

24. De Angelis M, Montemurno E, Piccolo M *et al.* Microbiota and metabolome associated with immunoglobulin A nephropathy (IgAN). *PLoS One* 2014; 9: e99006
25. Fellstrom BC, Barratt J, Cook H *et al.* Targeted-release budesonide versus placebo in patients with IgA nephropathy (NEFIGAN): a double-blind, randomised, placebo-controlled phase 2b trial. *Lancet* 2017; 389: 2117–2127
26. Ichinohe T, Pang IK, Kumamoto Y *et al.* Microbiota regulates immune defense against respiratory tract influenza A virus infection. *Proc Natl Acad Sci USA* 2011; 108: 5354–5359
27. McCarthy DD, Kujawa J, Wilson C *et al.* Mice overexpressing BAFF develop a commensal flora-dependent, IgA-associated nephropathy. *J Clin Invest* 2011; 121: 3991–4002
28. Oruc Z, Oblet C, Boumediene A *et al.* IgA structure variations associate with immune stimulations and IgA mesangial deposition. *J Am Soc Nephrol* 2016; 27: 2748–2761
29. Smith K, McCoy KD, Macpherson AJ. Use of axenic animals in studying the adaptation of mammals to their commensal intestinal microbiota. *Semin Immunol* 2007; 19: 59–69
30. Qin J, Li R, Raes J *et al.* A human gut microbial gene catalogue established by metagenomic sequencing. *Nature* 2010; 464: 59–65
31. Lechner SM, Abbad L, Boedec E *et al.* IgA1 protease treatment reverses mesangial deposits and hematuria in a model of IgA nephropathy. *J Am Soc Nephrol* 2016; 27: 2622–2629
32. Robert T, Berthelot L, Cambier A *et al.* Molecular insights into the pathogenesis of IgA nephropathy. *Trends Mol Med* 2015; 21: 762–775
33. Hooks KB, O'Malley MA. Dysbiosis and its discontents. *MBio* 2017; 8: pii: e01492-17
34. Piccolo M, De Angelis M, Lauriero G *et al.* Salivary microbiota associated with immunoglobulin A nephropathy. *Microb Ecol* 2015; 70: 557–565
35. Watanabe H, Goto S, Mori H *et al.* Comprehensive microbiome analysis of tonsillar crypts in IgA nephropathy. *Nephrol Dial Transplant* 2017; 32: 2072–2079
36. Schmitt R, Carlsson F, Morgelin M *et al.* Tissue deposits of IgA-binding streptococcal M proteins in IgA nephropathy and Henoch-Schönlein purpura. *Am J Pathol* 2010; 176: 608–618
37. De Palma G, Nadal I, Collado MC *et al.* Effects of a gluten-free diet on gut microbiota and immune function in healthy adult human subjects. *Br J Nutr* 2009; 102: 1154–1160
38. Cammarota G, Ianiro G, Tilg H *et al.* European consensus conference on faecal microbiota transplantation in clinical practice. *Gut* 2017; 66: 569–580

Received: 6.3.2018; Editorial decision: 17.9.2018